COMSOL Conference 2011 TOKYO
December 2, 2011, Tokyo, Japan

Excerpt from the Proceedings of the 2011 COMSOL Conference in Tokyo

Topology Optimization of Dielectric Metamaterials Based on the Level Set Method Using COMSOL Multiphysics

Masaki Otomori, Shinji Nishiwaki

Kyoto University, Kyoto, Japan, shinji@prec.kyoto-u.ac.jp

Abstract

This presentation shows a level set-based topology optimization method for the structural design of negative permeability dielectric metamaterials incorporating the level set boundary expression based on the concept of the phase field method, and its optimization algorithm implemented by COMSOL Multiphysics. Furthermore, several design examples are provided to confirm the usefulness of the proposed structural optimization method.

Keywards; Dielectric Metamaterials, Negative Permeability, Topology Optimization, Finite Element Method, Level Set Method,

1 Introduction

Electromagnetic metamaterials are artificial materials that exhibit extraordinary electromagnetic properties that are not available in nature. The characteristic property of electromagnetic metamaterials is a negative refractive index, that is, negative permittivity and permeability, which were first predicted by Veselago [1] in 1964. After Pendry *et al.* [2][3] and Smith *et al.* [4] showed some specific structures to realize these properties, considerable research was carried out to investigate the unusual properties of such materials and develop certain applications, such as cloaking devices [5], waveguides [6], leaky wave antennas [7], energy harvesting devices [8] and the like. Recently, new types of metamaterials that make use of the magnetic and electric resonance phenomena of dielectric materials have been proposed [9]-[15]. These dielectric metamaterials are expected to improve the manufacturability and to provide the possibility of achieving isotropic metamaterials under no metallic loss.

Metamaterials are usually composed of periodic arrays of unit cells which are adequately small compared to the desired wavelength. Electromagnetic metamaterial behaves as a material with negative properties, whereas the individual material do not. The effective property of metamaterials is obtained using a method such as the ones that compute the effective properties by averaging electric and magnetic fields in the unit cell [16], and by extracting of effective properties from S-parameters [17]-[20]. The basis of metamaterial unit cells can be designed using such effective property methods.

Several metamaterial designs have been proposed that achieve desirable performance at certain frequencies [21]. However, the design of unit cell significantly affects the metamaterials, so it is usually difficult or time-consuming to design an appropriate unit cell by trial and error methods. One systematic approach for the metamaterial design is to apply topology optimization method. Diaz and Sigmund [22] proposed a topology optimization method for the design of negative permeability metamaterials where several designs for metallic structures attached to dielectric plates that achieved negative permeability were provided. Sigmund [23] proposed a topology optimization method for dielectric metamaterials where the effective permeability were minimized at a specific frequency.

Since the performance of metamaterials is very sensitive to the presence of grayscale areas in the optimal configurations, an optimization method that provides configurations with clear boundaries is desirable. Recently, level set-based topology optimization methods have been proposed that fundamentally overcome the grayscale problem. In level set-based method, the structural boundaries are implicitly represented by iso-surface of the level set function, so clear optimized configurations can be obtained. Yamada et al. [24] proposed a level set-based topology optimization method incorporating the level set boundary expression based on the concept of the phase field method.

In this paper, we extended the above-mentioned level-set based topology optimization methods to the structural design of negative permeability dielectric metamaterials. The rest of this paper is as follows. Section 2 describes the level set-based topology optimization method, the formulation of the optimization problem for both two- and three-dimensional cases. Section 3 describes the numerical implementation

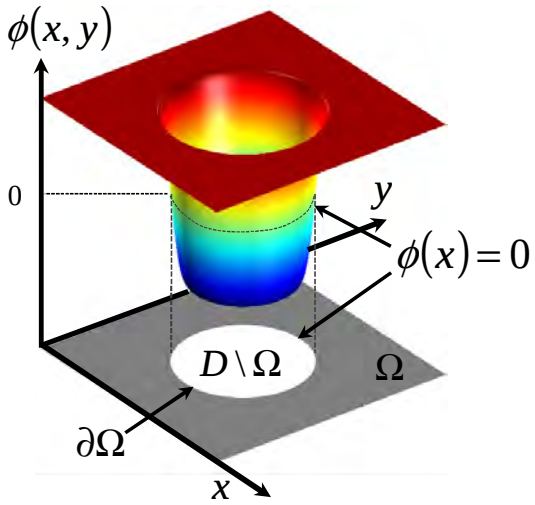

Figure 1: Fixed design domain D and level set function ϕ

which uses the Adjoint Variable Method (AVM) to obtain the sensitivity analysis. COMSOL multiphysics is used to solve the equillibrium and adjoint equation. Several design examples are provided for both two- and three-dimensional cases to confirm the validity of the presented method.

2 Formulations

2.1 Level set-based topology optimization method

Here, we briefly explain a level set-based topology optimization method incorporating a fictitious interface energy[24]. A topology optimization problem can be formulated using a fixed design domain D, which consists of a solid domain Ω, structural boundaries $\partial\Omega$ and a void domain $D\backslash\Omega$. As shown in Fig.1, in the level set method, the structural boundaries are implicitly represented using the iso-surface of the level set function, as follows.

$$\begin{cases} 1 \geq \phi(\mathbf{x}) > 0 & \text{for} \quad \forall \mathbf{x} \in \Omega \setminus \partial\Omega \\ \phi(\mathbf{x}) = 0 & \text{for} \quad \forall \mathbf{x} \in \partial\Omega \\ 0 > \phi(\mathbf{x}) \geq -1 & \text{for} \quad \forall \mathbf{x} \in D \setminus \Omega \end{cases} \tag{1}$$

where positive values of level set function represent the solid domain, negative values represent the void domain, and zero represents the structural boundaries. Let F be a objective function and G be a constraint functional, the optimization problem that minimizes objective functional is then formulated as follows using the above defined level set function ϕ.

$$\inf_{\chi_\phi} \quad F(\chi_\phi) = \int_D f_1(\mathbf{x}, \chi_\phi) \mathrm{d}\Omega + \int_\Gamma f_2(\mathbf{x}, \chi_\phi) \mathrm{d}\Gamma \tag{2}$$

$$\text{subject to} \quad G(\chi_\phi) = \int_D g(\mathbf{x}, \chi_\phi) \chi_\phi \mathrm{d}\Omega - G_{\max} \leq 0 \tag{3}$$

where f_1 and f_2 are density functions of the objective functional, g is density function of the constraint functional, and $G_{\max}$ is the upper limit of constraint functional. The characteristic function $\chi_\phi(\phi)$ is defined by following equation.

$$\chi_\phi(\phi) = \begin{cases} 1 & \text{if} \quad \phi \geq 0 \\ 0 & \text{if} \quad \phi < 0 \end{cases} \tag{4}$$

The above optimization problem is ill-posed problem because it allows the level set function to be discontinuous at everywhere. In this method, Tikhonov regularization method is used to regularize the

optimization problem. The above formulation is replaced with the following optimization problem:

$$\inf_{\phi} \quad F_R(\chi_\phi, \phi) = F + R \tag{5}$$

$$\text{subject to} \quad G(\chi_\phi) \leq 0, \tag{6}$$

where $R = \int_D \frac{1}{2}\tau \mid \nabla\phi \mid^2 \mathrm{d}\Omega$, and τ is a regularization parameter that adjusts the degree of regularization. Using Lagrange's method of undetermined multipliers, this formulation is then replaced with an optimization problem without constraints as follows.

$$\inf_{\phi} \quad \bar{F_R}(\chi_\phi, \phi) = \bar{F} + R, \tag{7}$$

where $\bar{F} = F + \lambda G$, $\bar{F_R}$ is the Lagrangian and λ is the Lagrange multiplier.

2.2 Updating scheme for level set function

Based on the above formulation, the KKT conditions of this optimization problem are described as follows:

$$\left\langle \frac{d\bar{F_R}}{d\phi}, \tilde{\phi} \right\rangle = 0, \quad \lambda G = 0, \quad \lambda \geq 0, \quad G \leq 0. \tag{8}$$

where the notation $\left\langle \frac{d\bar{F_R}}{d\phi}, \tilde{\phi} \right\rangle$ represents the Fréchet derivative of the regularized Lagrangian $\bar{F_R}$ with respect to ϕ.

Level set functions which satisfy the above KKT conditions are candidate solutions of the level set function that represent optimized configurations. However, it is not easy to find such level set functions directly. In this method, the optimization problem is replaced by a time evolution equation introducing a fictitious time t. The level set function is now updated by solving this equation, and an optimized configuration is obtained as follows. Here, we assume that the variation of the level set function is proportional to the gradient of Lagrangian $\bar{F_R}$, as follows:

$$\frac{\partial\phi}{\partial t} = -K(\phi)\frac{\delta\bar{F_R}}{\delta\phi}, \tag{9}$$

where $K > 0$ is a coefficient of proportionality. Substituting Eq.(7) into Eq.(9) and setting an appropriate boundary condition, we have the following reaction-diffusion equations.

$$\begin{cases} \dfrac{\partial\phi}{\partial t} = -K(\phi)\Big(\dfrac{\delta\bar{F}}{\delta\phi} - \tau\nabla^2\phi\Big) & \\ \dfrac{\partial\phi}{\partial n} = 0 & \text{on} \quad \partial D \setminus \partial D_N \\ \phi = 1 & \text{on} \quad \partial D_N \end{cases} \tag{10}$$

2.3 Electromagnetic wave propagation problem

2.3.1 Two-dimensional problem

Here, we explain the two-dimensional design problem for dielectric metamaterials. Figure 2 shows the design domain. Transverse magnetic (TM) waves propagate in x-y direction where the magnetic field vector is polarized orthogonal to the wave direction. Incident waves enter the domain from the input boundary Γ_1 and output waves are observed at the output boundary Γ_2. Under periodic conditions, the upper and lower boundaries Γ_{PEC} are set to Perfectly Electric Conductors (PEC). In the two-dimensional case, the governing equation is given as the following equations. The relative permeability of both the background material and the dielectric material is set to 1.

$$a(H_z, \tilde{H_z}) = l(\tilde{H_z}) \quad \text{for} \quad H_z \in U, \quad \tilde{H_z} \in U \tag{11}$$

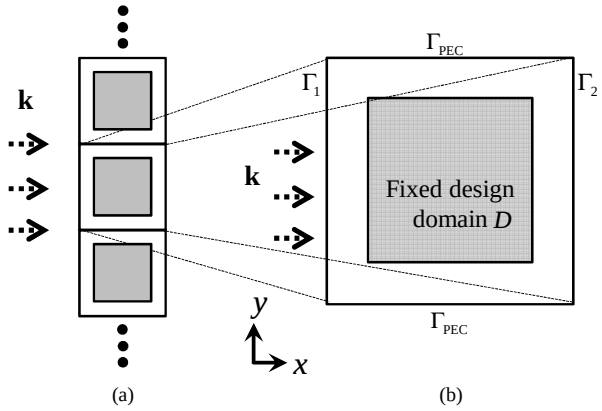

Figure 2: (a) Periodic structure for three-dimensional problem; (b) design domain and boundary conditions

where

$$a(H_z, \tilde{H}_z) = \int_D \nabla \tilde{H}_z \cdot \left(\epsilon_r^{-1} \nabla H_z\right) d\Omega - k_0^2 \int_D \tilde{H}_z H_z d\Omega + jk_0 \int_{\Gamma_1+\Gamma_2} \tilde{H}_z H_z d\Gamma \tag{12}$$

$$l(\tilde{H}_z) = 2jk_0 \int_{\Gamma_1} H_z^i \tilde{H}_z d\Gamma \tag{13}$$

$$U = \{\tilde{H}_z \in H^1(\Omega)\}. \tag{14}$$

where ϵ_r is the relative permittivity, $k_0 = \omega\sqrt{\epsilon_0 \mu_0}$ is the wave number in a vacuum and H^i is an incident wave.

2.3.2 Three-dimensional problem

Here, we explain the three-dimensional electromagnetic wave propagation problem. Figure 3 shows the design domain for the three-dimensional problem. Incident waves enter the domain from the input boundary Γ_1. Under periodic conditions, the upper and lower boundaries Γ_{PEC} are set as Perfectly Electric Conductors (PEC) and the front and rear boundaries Γ_{PMC} are set as Perfectly Magnetic Conductors (PMC). Here, the gorverming equation is given as the following equations. Again, the relative permeability of both the background material and the dielectric material is again set to 1.

$$a(\mathbf{E}, \tilde{\mathbf{E}}) = l(\tilde{\mathbf{E}}) \quad \text{for} \quad \mathbf{E} \in U, \quad \tilde{\mathbf{E}} \in U, \tag{15}$$

where

$$a(\mathbf{E}, \tilde{\mathbf{E}}) = \int_D \left(\nabla \times \tilde{\mathbf{E}}\right) \cdot (\nabla \times \mathbf{E})\, d\Omega - k_0^2 \int_D \epsilon_r \tilde{\mathbf{E}} \cdot \mathbf{E} d\Omega + jk_0 \int_{\Gamma_1+\Gamma_2} \tilde{\mathbf{E}} \cdot [\mathbf{n} \times (\mathbf{E} \times \mathbf{n})]\, d\Gamma \tag{16}$$

$$l(\tilde{\mathbf{E}}) = 2jk_0 \int_{\Gamma_1} \tilde{\mathbf{E}} \cdot \mathbf{E}^i d\Gamma \tag{17}$$

$$U = \{\tilde{\mathbf{E}} \in H^1(\Omega)\}. \tag{18}$$

where $\mathbf{E}^i$ is the incident field and $\mathbf{n}$ is the normal vector.

2.4 Effective permeability

Here, we explain the method for obtaining an effective property. Several approaches were proposed to compute these effective properties. These methods are typically categorized into two types. One approach is to average the electric and magnetic fields in a unit cell [16], and the other is to compute the effective properties based on the coefficient of the S-parameter, namely, the complex reflectivity and complex permeability [17]-[20]. Considering the accuracy of the methods and the ease of implementions, we use

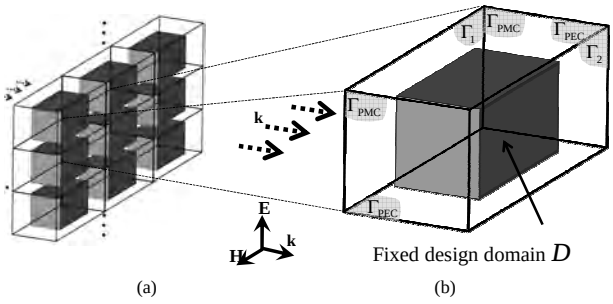

Figure 3: (a) Periodic structure for three-dimensional problem; (b) design domain and boundary conditions

the extended approach [20] of original S-parameter-based method [17], where the effective parameters are computed based on S-parameters.The effective permeability μ_{eff} is then obtained by following equation.

$$\mu_{\text{eff}} = Zn, \tag{19}$$

where

$$Z = \sqrt{\frac{(1+S_{11})(1+S_{22}) - S_{21}^2}{(1-S_{11})(1-S_{22}) - S_{21}^2}}, \tag{20}$$

$$n = \cos^{-1}\left(\frac{\beta}{2S_{21}}\right)\frac{\lambda}{2\pi d}, \tag{21}$$

and

$$\beta = 1 + S_{11}S_{22} - S_{21}^2. \tag{22}$$

In above formulation, S_{22} is used in addition to S_{11} and S_{21}, for inhomogeneous inclusions. We note that symmetric optimized configurations can be obtained using this formulation because it is symmetric with respect to S_{11} and S_{22}.

2.5 Formulation of optmization problem

2.5.1 Effective permeability minimization problem

Here, we discuss the effective permeability minimization problem. One particularly interesting optimization problem is to obtain metamaterial designs that exhibit extreme negative permeability values. The optimization problem objective is here to find a dielectric material distribution within the fixed design domain that minimizes the effective permeability. Figure 4(a) shows a typical effective permeability curve, where μ' and μ'' show the real and imaginary part of the effective permeability. The real part of the effective permeability has positive peak and anti-resonance point. The effective permeability has a desirable negative value at this anti-resonance point. The purpose of the optimization is to minimize the real part of the effective permeability at a desired frequency. However, if the positive peak lies between the initial anti-resonance point and the target frequency, namely, if the target frequency is in the hatched area for the case shown in Fig.4(a), configurations that demonstrate negative real part of effective permeability is impossible to obtain directly. Thus, a two-step optimization process is used as in reference [23], where, taking advantage of the fact that the imaginary part does not have positive peak, the imaginary part μ'' of permeability is minimized during the first step (Fig.4(b)). After that, the real part of the effective permeability is minimized during the second step (Fig.4(c)), using the optimized configuration obtained in the first step as the initial configuration.

The optimization problem for this first step is described as follows.

$$\inf_{\phi} \qquad F = \mu'' \tag{23}$$

$$\text{subject to} \quad G \leq 0 \tag{24}$$

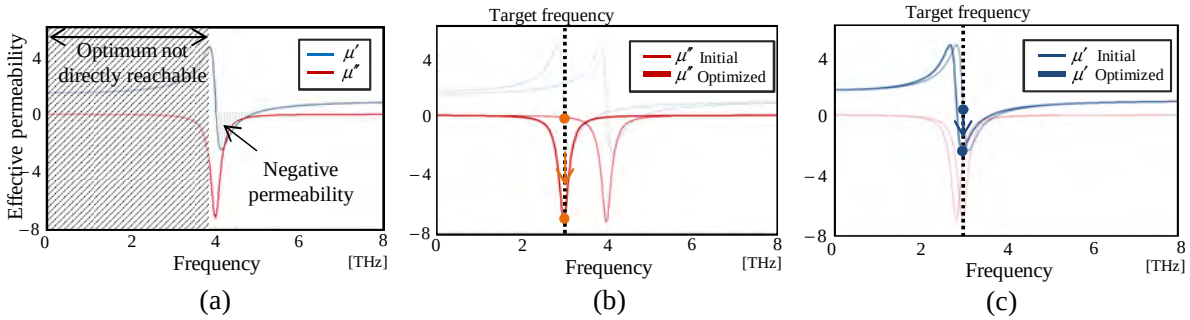

Figure 4: (a) A typical effective permeability curve; (b) the imaginary part of effective permeabiliy is minimized during the first step; (c) the real part of effective permeability is minimized during second step

The optimization problem for the second step is described as follows.

$$\inf_{\phi} \quad F = \mu' \tag{25}$$

$$\text{subject to} \quad G \leq 0 \tag{26}$$

2.5.2 Effective permeability design problem

Here, we discuss the effective permeability design problem. Obtaining the metamaterial design that demonstrate a certain desirable value for the effective permeability is of great importance to some novel devices. The optimization problem objective is to find a dielectric material distribution that demonstrate the desired value of effective permeability. The purpose of the optimization here is to obtain a distribution of dielectric material which demonstrate the prescribed value of effective permeability at a desired frequency. The optimization problem can be formulated to minimize the square of the difference between the effective permeability and a prescribed value. Again, the two-step optimization process is used. The imaginary part is minimized during the first step, and the square of the difference between the effective permeability and a prescribed value is minimized during the second step. The optimization problem for the second step can be formulated as follows.

$$\inf_{\phi} \quad F = (\mu' - \mu'_{\text{tar}})^2 \tag{27}$$

$$\text{subject to} \quad G \leq 0 \tag{28}$$

2.6 Sensitivity Analysis

2.6.1 Two-dimensional case

Now, we discuss the sensitivity analysis for a two-dimensional case. The sensitivities are obtained using the Adjoint Variable Method (AVM). First, the Lagrangian of the optimization problem is formulated as follows.

$$\bar{F} = F(\phi) - \sum_{ij=11,21,22} \frac{\partial F}{\partial S_{ij}} \left(a(H_z, \tilde{H}_{z,ij}) - L(\tilde{H}_{z,ij}) \right), \tag{29}$$

where $\tilde{H}_{z,ij}$ denotes the adjoint variables with respect to S_{ij}. The sensitivity of the Lagrangian is then obtained using the AVM.

$$\begin{aligned} \left\langle \frac{d\bar{F}}{d\phi}, \tilde{\phi} \right\rangle &= \sum_{ij=11,21,22} \frac{\partial F}{\partial S_{ij}} \left\langle \frac{\partial S_{ij}}{\partial \mathbf{E}}, \tilde{\mathbf{E}} \right\rangle \left\langle \frac{\partial \mathbf{E}}{\partial H_z}, \tilde{H}_{z,ij} \right\rangle - \sum_{ij=11,21,22} \frac{\partial F}{\partial S_{ij}} \left(\left\langle \frac{\partial a}{\partial H_z}, \tilde{H}_{z,ij} \right\rangle + \left\langle \frac{\partial a}{\partial \phi}, \tilde{\phi} \right\rangle \right) \\ &= - \sum_{ij=11,21,22} \frac{\partial F}{\partial S_{ij}} \left\langle \frac{\partial a}{\partial \phi}, \tilde{\phi} \right\rangle, \end{aligned} \tag{30}$$

where the adjoint variable $\tilde{H}_{z,ij}$ is obtained by solving the adjoint equation described as follows.

$$\left\langle \frac{\partial S_{ij}}{\partial \mathbf{E}}, \tilde{\mathbf{E}} \right\rangle \left\langle \frac{\partial \mathbf{E}}{\partial H_z}, \tilde{H}_{z,ij} \right\rangle - \left\langle \frac{\partial a}{\partial H_z}, \tilde{H}_{z,ij} \right\rangle = 0. \tag{31}$$

2.6.2 Three-dimensional case

Here, we discuss the sensitivity analysis for a three-dimension case. The Lagrangian of the optimization problem is formulated as follows.

$$\bar{F} = F - \sum_{ij=11,21,22} \frac{\partial F}{\partial S_{ij}} \left(a(\mathbf{E}, \tilde{\mathbf{E}}_{ij}) - L(\tilde{\mathbf{E}}_{ij}) \right), \tag{32}$$

where $\tilde{\mathbf{E}}_{ij}$ denotes the adjoint variables with respect to S_{ij}. The sensitivity of the Lagrangian is obtained, again using the AVM.

$$\begin{aligned} \left\langle \frac{d\bar{F}}{d\phi}, \tilde{\phi} \right\rangle &= \sum_{ij=11,21,22} \frac{\partial F}{\partial S_{ij}} \left\langle \frac{\partial S_{ij}}{\partial \mathbf{E}}, \tilde{\mathbf{E}}_{ij} \right\rangle - \sum_{ij=11,21,22} \frac{\partial F}{\partial S_{ij}} \left(\left\langle \frac{\partial a}{\partial \mathbf{E}}, \tilde{\mathbf{E}}_{ij} \right\rangle + \left\langle \frac{\partial a}{\partial \phi}, \tilde{\phi} \right\rangle \right) \\ &= - \sum_{ij=11,21,22} \frac{\partial F}{\partial S_{ij}} \left\langle \frac{\partial a}{\partial \phi}, \tilde{\phi} \right\rangle, \end{aligned} \tag{33}$$

where the adjoint variable $\tilde{\mathbf{E}}_{ij}$ is obtained by solving the adjoint equation described as follows.

$$S_{ij} - a\left(\mathbf{E}, \tilde{\mathbf{E}}_{ij}\right) = 0. \tag{34}$$

3 Numerical implementations

3.1 design variable

3.1.1 Two-dimensional case

For two-duimensional case, the relative permittivity ϵ_r in the domain is defined using the reciprocal of the relative permittivity of solid and void domain.

$$\epsilon_r^{-1} = \left(\epsilon_1^{-1} - \epsilon_0^{-1}\right) H(\phi) + \epsilon_0^{-1}, \tag{35}$$

where ϵ_1 is the relative permittivity of the dielectric material, ϵ_0 is the relative permittivity of the background material, and $H(\phi)$ is the Heaviside function.

The purpose of the reciprocal formulation used in Eq.(35) is to stabilize the optimization calculations. We note that the reciprocal formulation and the linear formulation respectively represent lower and upper theoretical bounds of the effective properties of the composite materials investigated here [25], so the reciprocal formulation is physically reasonable .

In optimization process, the following smoothed Heaviside function is used.

$$H(\phi) = \begin{cases} 0 & (\phi < -w) \\ \frac{1}{2} + \frac{\phi}{w}\left(\frac{15}{16} - \frac{\phi^2}{w^2}\left(\frac{5}{8} - \frac{3}{16}\frac{\phi^2}{w^2}\right)\right) & (-w \le \phi < w) \\ 1 & (w \le \phi), \end{cases} \tag{36}$$

where w is the transition width of the Heaviside function which is set to a sufficiently small value.

3.1.2 Three-dimensional case

For three-dimensional case, the relative permittivity ϵ_r is defined using the linear formulation.

$$\epsilon_r = (\epsilon_1 - \epsilon_0) H(\phi) + \epsilon_0. \tag{37}$$

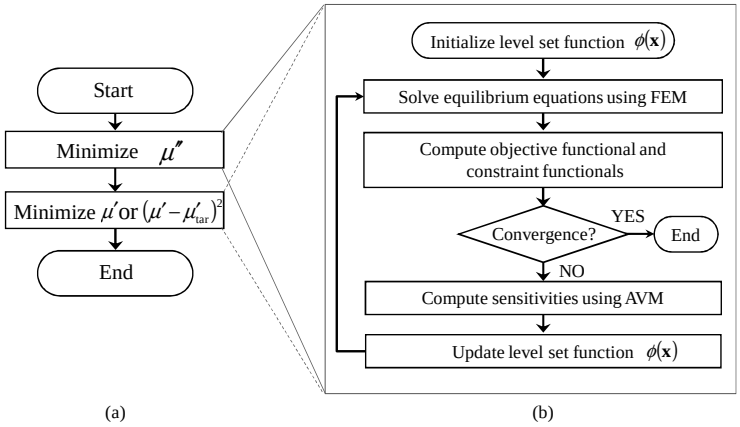

Figure 5: (a) Flowchart of optimization algorithm; (b)flowchart for optimization algorithm steps

3.2 Optimization algorithm

Fig.5(a) shows the optimization flowchart. During the first step, the imaginary part of the effective permeability is minimized. Then during the second step, the real part of the effective permeability is minimized for the effective permeability minimization problem. The square of the difference between the real part of the effective permeability and the target value of the effective permeability is minimized in the effective permeability design problem. Fig.5(b) shows the optimization flowchart for each step. First, the level set function is initialized, then the equilibrium equation is solved using the Finite Element Method (FEM) and the objective and constraint functional are computed. If the objective functional has converged, the optimization procedure terminates, and if not, the sensitivities of objective and constraint functional are computed using the AVM. Then the level set function is updated by solving the reaction diffusion equation and the process returns to the second step. COMSOL Multiphysics is used to solve the equilibrium and adjoint equation, and compute the objective and constraint functional.

4 Numerical examples

Numerical examples for two- and three-dimensional negative permeability dielectric metamaterials design problems are now presented to confirm the validity of the presented method.

4.1 Two-dimensional design problems

Here, we first discuss effective permeability minimization problems where the target frequencies are set either higher or lower than that of the positive peak of the initial configuration, to examine whether the optimization can successfully find optimized configurations independent of the location of the positive peak of the initial configuration. Next, we discuss an effective permeability design problem to find an optimized configuration that exhibits a prescribed value of the effective permeability. Figure 6 shows the design domain and boundary conditions. The size of the analysis domain is set to 120μm $\times$ 120μm and the size of the fixed design domain is set to 80μm $\times$ 80μm. The whole domain is discretized using 120 $\times$ 120 square elements. The relative permittivity ϵ_1 of the dielectric material is set to $100 - 1i$ and the relative permittivity ϵ_0 of the background material is set to 1. The transition width w of the Heaviside function is set to 0.001.

4.1.1 Effective permeability minimization problem 1

Here, the target frequency is set to 0.30THz to examine a case where the target frequency is lower than where the anti-resonance point of the initial configuration occurs. The upper limit of the volume fraction is set to 70%.

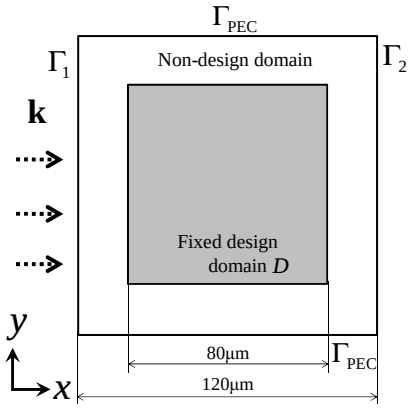

Figure 6: Design domain and boundary conditions for two-dimensional problem

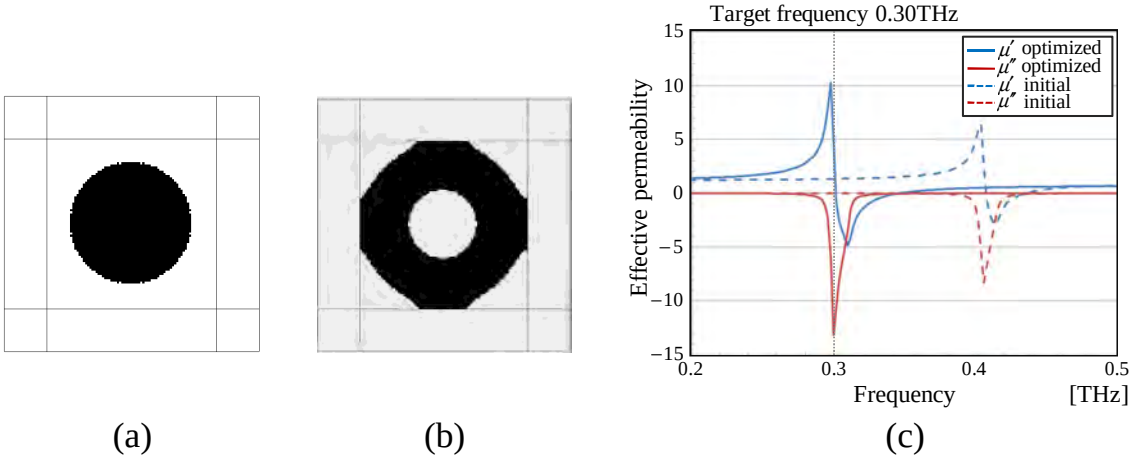

Figure 7: Optimization results of the first step for two-dimensional effective permeability minimization problem 1: (a) initial configuration; (b) optimized configuration; (c) Effective permeability curve

Figure 7 shows the initial and optimized distribution obtained in the first step, and the obtained effective permeability curves of the initial and optimized distribution. The frequency at the anti-resonance point of the imaginary part of the effective permeability gradually decreases during the optimization procedure and finally reaches the prescribed frequency. The value of the imaginary part of the effective permeability of the initial configuration and optimization configuration at 0.30THz is respectively, -0.01, -13.19. The real part of the effective permeability is then minimized during the second step of the optimization procedure. Figure 8 shows the initial and optimized configuration obtained in the second step, and the effective permeability curve of the initial and optimized distribution. The values of the real part of the effective permeability of the initial configuration of the first step and optimized configuration obtained in the second step at 0.30THz are respectively 1.33 and -5.07. It shows that the optimization successfully finds an optimized solution that has negative effective permeability.

Figure 9 shows the electric field of the initial configuration after the first step, and the optimized configuration obtained after the second step. The red arrows in the figure indicate the electric field. It shows that a circular electric field is generated in the optimized design, which induces a magnetic field along the z-axis.

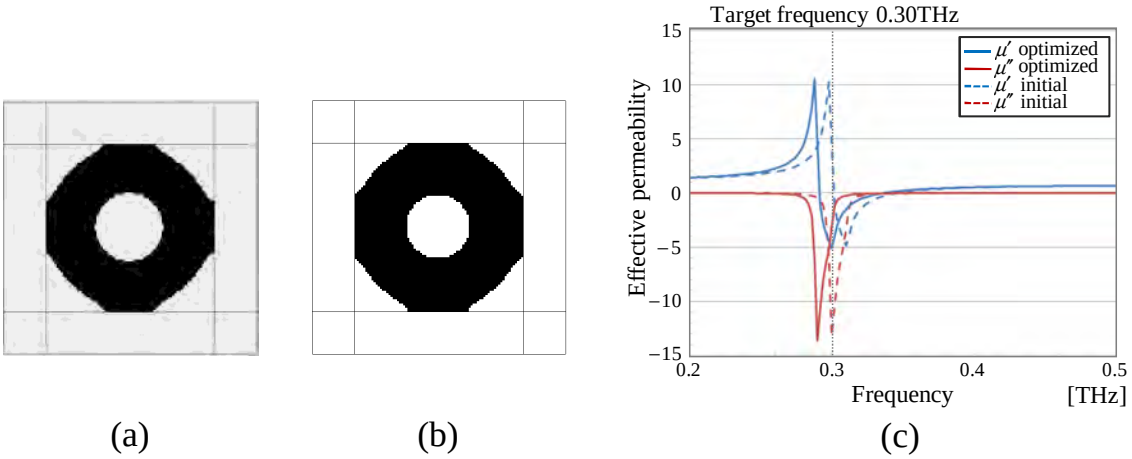

Figure 8: Optimization results of the second step for two-dimensional effective permeability minimization problem 1: (a) initial configuration; (b) optimized configuration; (c) Effective permeability curve

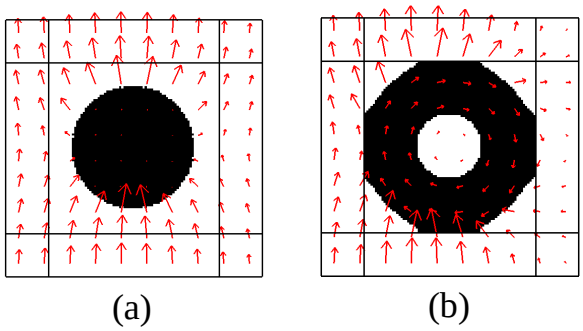

Figure 9: Configurations and electric field distribution for two-dimensional effective permeability minimization problem 1: (a) initial; (b) optimized

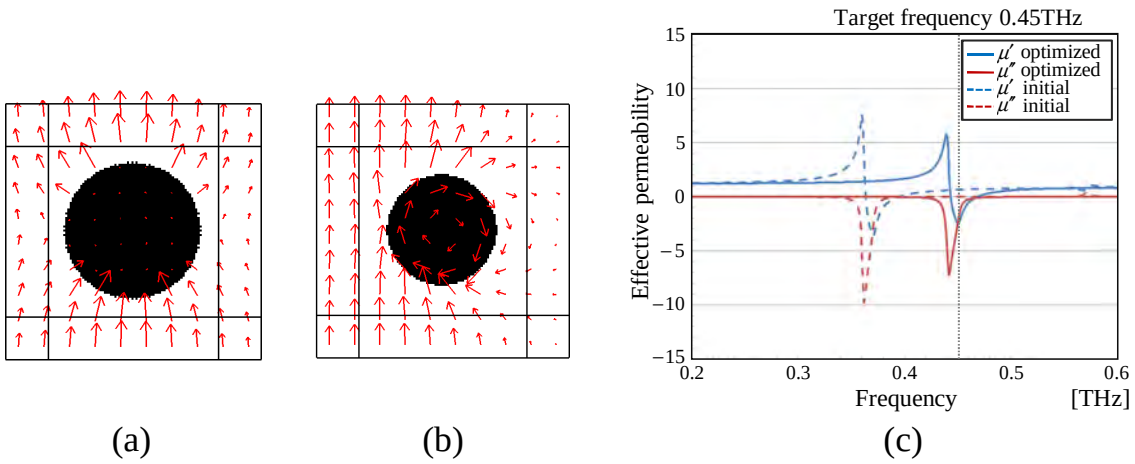

Figure 10: Optimization results for two-dimensional effective permeability minimization problem 2: (a) initial configuration; (b) optimized configuration; (c) Effective permeability curve

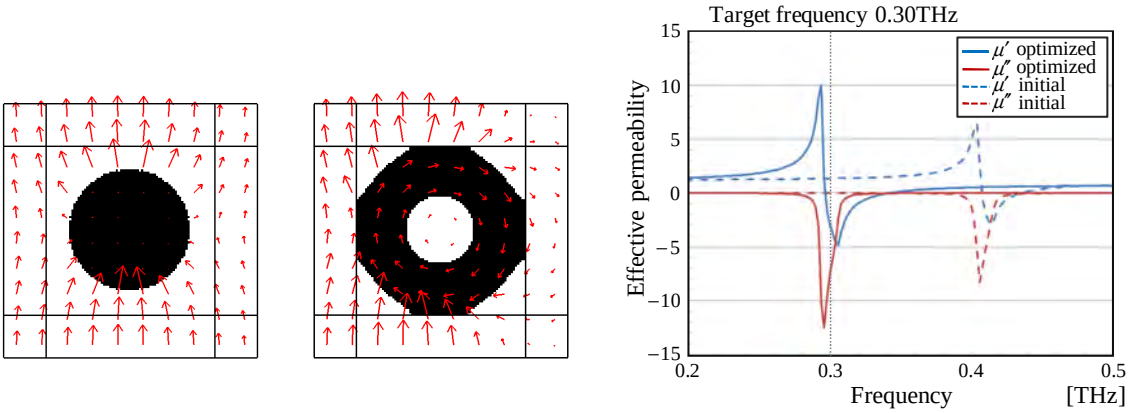

Figure 11: Optimization results for two-dimensional effective permeability design problem: (a) initial configuration; (b) optimized configuration; (c) Effective permeability curve

4.1.2 Effective permeability minimization problem 2

Here, the target frequency is set to 0.45THz to examine a case where the target frequency is higher than that of the anti-resonance point of the initial configuration. A volume constraint is not applied here.

Figure 10 shows the initial and optimized configurations, and electric field distribution obtained in the second step of the optimization procedure. Figure 10 shows the corresponding effective permeability curves for the initial and optimized distribution. The real part of the effective permeability of the initial and optimized configuration at 0.45THz is, respectively, 0.65 and -2.44, which shows that the optimization successfully finds an optimized solution that exhibits negative effective permeability. The red arrows in Fig.10 show the electric field, and we again see that a circular electric field is generated in the center of the design domain of the optimized configuration.

4.1.3 Effective permeability design problem

Next, we shows an effective permeability design problem. Here, the target frequency is set to 0.30THz and the target value for the effective permeability is set to -3.0. The upper limit of the volume fraction is set to 70%. As described in previous chapter, the imaginary part of effective permeability is minimized during the first step, then the square of the difference between the effective permeability and a prescribed value is minimized during the second step of the optimization process.

Fig. 11 shows the initial and optimized configurations, and electric field distributions obtained in the second step. Figure 11 shows the effective permeability curves of the initial and optimized distribution obtained in the second step. The real part of the effective permeability of the optimized configuration at 0.30THz is -3.00, which indicates that the optimization successfully finds an optimized configuration that has a desirable value for the effective permeability at the target frequency.

4.2 Three-dimensional problems

Here, we discuss a three-dimensional design problem. Figure 12 shows the design domain and boundary conditions. The size of the analysis domain is set to 120μm $\times$ 120μm $\times$ 150μm and the size of the fixed design domain is set to 80μm $\times$ 80μm $\times$ 110μm. The analysis domain is discretized using $48 \times 48 \times 60$ square elements. The relative permittivity ϵ_1 of the dielectric material is set to $100 - 1i$ and the relative permittivity ϵ_0 of the background material is set to 1. The transition width w of the Heaviside function is set to 0.001.

4.2.1 Effective permeability minimization problem

The effective permeability minimization problem where the target frequency is set to 0.30THz examines a case where the target frequency is lower than that of the anti-resonance point of the initial configuration.

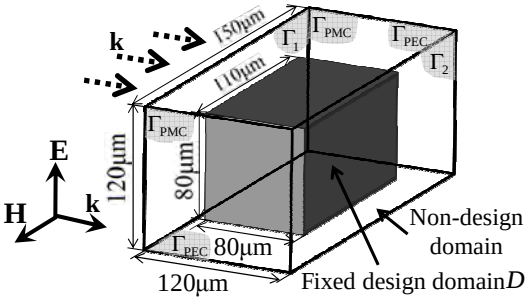

Figure 12: Design domain and boundary conditions for three-dimensional design problem

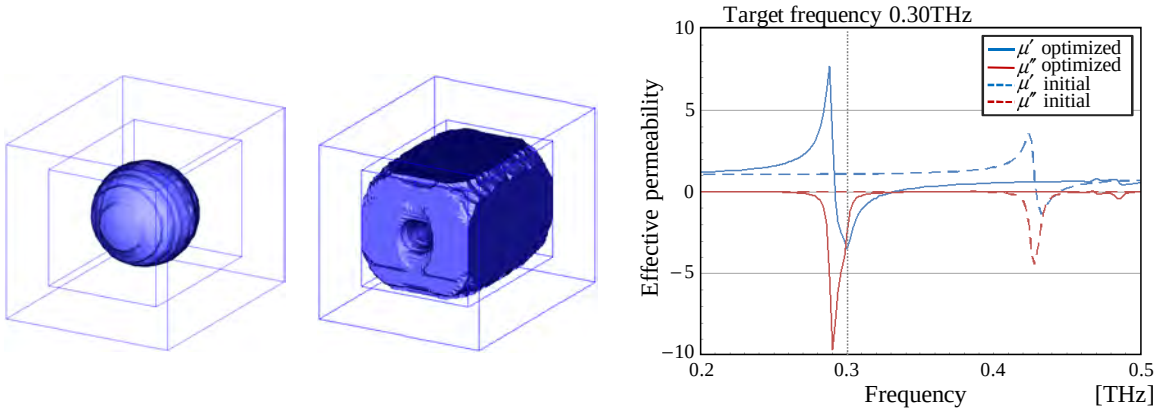

Figure 13: Optimization results for three-dimensional effective permeability minimization problem: (a) initial configuration; (b) optimized configuration; (c) Effective permeability curve

A spherical shape with a volume fraction of 25% is used as the initial configuration. The upper limit of the volume fraction is set to 90%.

The initial and optimized distribution obtained in the second step of the optimization process are shown in Fig. 13 and the corresponding effective permeability curves are shown in Fig. 13. The anti-resonance point of the real part of the effective permeability gradually decreases during the optimization procedure and finally reaches the prescribed frequency at the end of the optimization procedure. The real part of the effective permeability of the initial and optimized configuration at 0.30THz are respectively 1.06 and -3.49, which shows that the optimization can successfully find an optimized solution that demonstrates negative effective permeability.

5 Conclusions

This paper discussed a topology optimization method of dielectric metamaterials based on the level set method using COMSOL multiphysics. The optimization problems were formulated for both two- and three-dimensional problem to minimize the effective permeability, and to obtain a prescribed effective permeability at a target frequency. A level set-based boundary expression was applied to obtain clear boundaries, and an S-parameter-based approach was applied to compute the effective permeability of the metamaterials. Based on the formulation of the optimization problem, an optimization algorithm was constructed. COMSOL multiphysics was used to solve the electromagnetic wave problems and adjoint equation to obtain the sensitivity analysis. Several design examples were provided to examine the validity

of presented method. We also confirm that the presented method obtains smooth and clear optimized configurations for all the presented cases.

References

[1] V. G. Veselago, The electrodynamics of substances with simultaneously negative values of ϵ and μ, Soviet Physics Uspekhi, 10 (4) (1968) 509–514.

[2] J. B. Pendry, A. J. Holden, W. J. Stewart and I. Youngs, Extremely low frequency plasmons in metallic mesostructures, Physical Review Letters, 76 (25) (1996) 4773–4776.

[3] J. B. Pendry, A. J. Holden, D. J. Robbins and W. J. Stewart, Magnetism from conductors and enhanced nonlinear phenomena, IEEE Transactions on Microwave Theory and Techniques, 47 (11) (1999) 2075–2084.

[4] D. R. Smith, W. J. Padilla, D. C. Vier, S. C. Nemat-Nasser and S. Schultz, Composite medium with simultaneously negative permeability and permittivity, Physical Review Letters, 84 (18) (2000) 4184–4187.

[5] D. Schurig, J. J. Mock, B. J. Justice, S. A. Cummer, J. B. Pendry, A. F. Starr, and D. R. Smith, Metamaterial electromagnetic cloak at microwave frequencies, Science, 314 (5801) (2006) 977–980.

[6] S. Hrabar, J. Bartolic and Z. Sipus, Waveguide minimization using uniaxial negative permeability metamaterial, IEEE Transactions on Antennas and Propagation, 53 (1) (2005) 110–119.

[7] C. Caloz, T. Itoh and A. Rennings, CRLH metamaterial leaky-wave and resonant antennas, IEEE Antennas and Propagation Magazine, 50 (5) (2008) 25–39.

[8] Q. Cheng, T. J. Cui, W. X. Jiang and B. G. Cai, An omnidirectional electromagnetic absorber made of metamaterials, New Journal of Physics, 12 (2010) 063006.

[9] C. L. Holloway, E. F. Kuester, J. Baker-Jarvis and P. Kabos, A double negative (DNG) composite medium composed of magnetodielectric psherical particles embedded in a matrix, IEEE Transaction on Antennas and Propagation, 51 (10) (2003) 2596–2603.

[10] A. Ahmadi and H. Mosallaei, Physical configuration and performance modeling of all-dielectric metamaterials, Physical Review B, 77 (4) (2008) 045104

[11] Q. Zhao, J. Zhou, F. Zhang and D. Lippens, Mie resonance-based dielectric metamaterials, Materials Today, 12 (12) (2009) 60–69.

[12] L. Peng, L. Ran, H. Chen, H. Zhang, J. A. Kong and T. M. Grzegorczyk, Experimental observation of left-handed behavior in an array of standard dielectric resonators, Physical Review Letters, 98 (15) (2007) 157403.

[13] K. Shibuya, K. Takano, N. Matsumoto, K.Izumi, H. Miyazaki, Y. Jimba and M. Hangyo, Terahertz metamaterials composed of TiO_2 cube arrays, Proceedings of the 2nd International Congress on Advanced Electromagnetic Materials in Microwaves and Optics, Pamplona, Spain, September 21-26, 2008.,

[14] W. Cai, U. K. Chettiar, A. V. Kildishev and V. M. Shalaev, Designs for optical cloaking with high-order transformations, Optics Express, 16 (8) (2008) 5444–5452.

[15] T. Ueda, N. Michishita, M. Akiyama and T. Itoh, Dielectric-resonator-based composite right/left-handed transmission lines and their application to leaky wave antenna, IEEE Transactions on Microwave Theory and Techniques, 56 (10) (2008) 2259–2269.

[16] D. R. Smith and J. B. Pendry, Homogenization of metamaterials by field averaging, Journal of the Optical Society of America B, 23 (3) (2006) 391–403.

[17] D. R. Smith, S. Schultz, P. Markoš and C. M. Soukoulis, Determination of effective permittivity and permeability of metamaterials from reflection and transmission coefficients, Physical Review B, 65 (19) (2002) 195104. s

[18] X. Chen, T. M. Grzegorczyk, B. I. Wu, J. Jr. Pacheco and J. A. Kong, Robust method to retrieve the constitutive effective parameters of metamaterials, Physical Review E, 70 (1) (2004) 016608.

[19] G. Lubkowski, R. Schuhmann and T. Weiland, Extraction of effective metamaterial parameters by parameter fitting of dispersive models, Microwave and Optical Technology Letters, 49 (2) (2007) 285–288.

[20] D. R. Smith, D. C. Vier, T. Koschny and C. M. Soukoulis, Electromagnetic parameter retrieval from inhomogeneous metamaterials, Physical Review E, 71 (3) (2005) 036617.

[21] C. M. Soukoulis, S. Linden and M. Wegener, Negative refractive index at optical wavelengths, Science, 315 (5808) (2007), 47–49.

[22] A. R. Diaz and O. Sigmund, A topology optimization method for design of negative permeability metamaterials, Structural and Multidisciplinary Optimization, 41 (2) (2010) 163–177.

[23] O. Sigmund, Systematic design of metamaterials by topology optimization, IUTAM Symposium on Modelling Nanomaterials and Nanosystems, R. Pyrz and J. C. Rauhe (eds.), Springer, Netherlands, 13 (2009) 151–159.

[24] T. Yamada, K. Izui, S. Nishiwaki and A. Takezawa, A topology optimization method based on the level set method incorporating a fictitious interface energy, Computer Methods in Applied Mechanics and Engineering, 199 (45-48) (2010) 2876–2891.

[25] D. J. Bergman, The dielectric constant of a composite material - a problem in classical physics, Physics Reports, 43 (9) (1978) 377–407.